Momentum noise in vacuum tunneling transducers

B. Yurke and G. P. Kochanski
AT&T Bell Laboratories, Murray Hill, New Jersey 07974-2070
(Received 15 November 1989)

The vacuum tunneling probe can serve as a sensitive transducer of position into current. The performance of such a transducer is characterized by both the uncertainty in the inferred position Δx and the uncertainty in the momentum transfer Δp during the measurement. For realistic barrier parameters we find that the uncertainty product $\Delta x\,\Delta p$ differs by less than 1% from $\hbar/2$. We also calculate the expectation values of the force associated with tunneling electrons. If sufficiently sensitive force measurements can be made, this force can provide information about a surface or an absorbed atom, differing from that provided by the tunneling current.

I. INTRODUCTION

Recently, Bocko, Stephenson, and Koch[1] have pointed out that the vacuum tunneling probe used in the scanning tunneling microscope[2-4] represents a new class of nonreciprocal electromechanical transducers. They argue that such a probe may reach the quantum limit for a measurement of the position of a macroscopic mechanical oscillator even when followed by non-quantum-limited amplifiers.

In their noise analysis, it is assumed that when performing a position measurement, the tunneling electrons induce a momentum uncertainty $\Delta p \cong \hbar/\Delta x$, where Δx is the uncertainty in the inferred position of the mass. Here we rigorously show that an uncertainty product $\Delta x\,\Delta p = \hbar/2$ can be realized for a square-well barrier. For a realistic barrier we find that the uncertainty product differs by less than 1% from $\hbar/2$. Although carried out only for one-dimensional barriers, the analysis suggests that real vacuum tunneling position transducers could come close to achieving the minimum allowed by quantum mechanics for the uncertainty product of position and momentum.

The noise analysis of Bocko *et al.*[1] suggests that it may be feasible to measure the quantum fluctuations, Δp, in the momentum transferred across the vacuum barrier. If such a sensitivity can be achieved, an atomic force microscope[3,5,6] could be used to probe directly the exchange force that results as electrons tunnel across the vacuum barrier. These forces are the covalent-bonding forces between the two sides of the tunnel junction. Momentum-transfer measurements could thus complement more usual methods[7,8] of extracting the physical and chemical properties of surfaces via tunneling microscopy. As an illustration, we have calculated the momentum transfer for a square-well atom on the surface of the tunneling probe.

II. CURRENT OPERATORS

Tunneling theory has concentrated on evaluating the charge transported across a barrier.[9-11] Here, in addition, we evaluate the momentum transported across a barrier. Expressions for the second-quantized current and momentum-current operators will be obtained. The current and momentum shot noise is characterized by the variances of these operators. For simplicity, the analysis will be confined to one-dimensional barriers.

Consider the case where the electron wave function satisfies the equation:

$$i\hbar\frac{\partial\psi}{\partial t} = -\frac{\hbar^2}{2m}\frac{\partial^2\psi}{\partial x^2} + V(x)\psi\ . \tag{2.1}$$

For simplicity, the potential $V(x)$ will have the form depicted in Fig. 1. The potential is taken to be constant for $x < l_1$ or $x > l_2$,

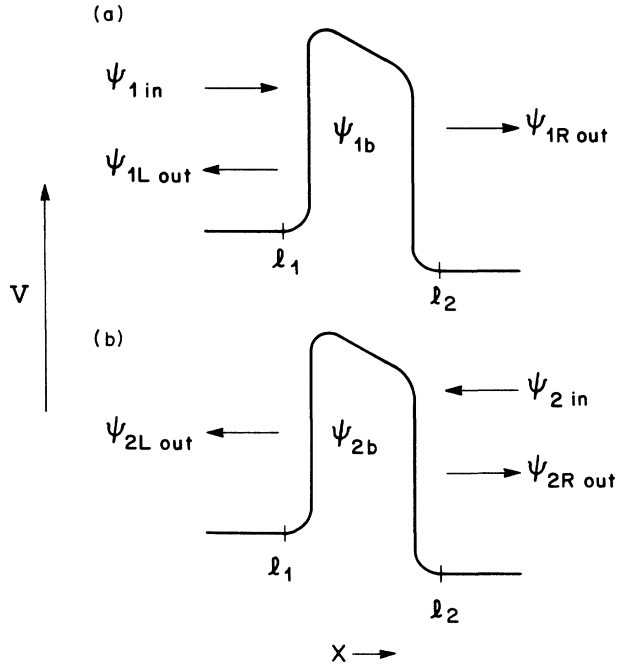

FIG. 1. A barrier potential. The figure indicates the behavior of two independent solutions to the Schrödinger equation. In (a) the incoming wave propagates toward the barrier from the left. In (b) the incoming wave propagates toward the barrier from the right.

$$V(x)=\begin{cases} V_1 & \text{for } x<l_1 \ , \\ V_2 & \text{for } x>l_2 \ . \end{cases} \tag{2.2}$$

The region $l_1 \le x \le l_2$ is the barrier. We will leave $V(x)$ unspecified here and do as much of the calculation as possible in terms of the scattering matrix.

In the region $x<l_1$ and $x>l_2$, the energy eigenstates $\psi_E(x,t)=\psi_E(x)e^{-iEt/\hbar}$ will consist of sums of plane waves of the form

$$\psi_E(x)=A_k e^{ikx}+B_k e^{-ikx} \ . \tag{2.3}$$

We introduce the notation

$$k_i=[(2m/\hbar^2)(E-V_i)]^{1/2} \ , \tag{2.4}$$

where $i \in \{1,2\}$ refers to space beyond the left or right sides of the barrier. It is convenient to work with the two independent solutions, $\psi_1(k_2,x)$ and $\psi_2(k_2,x)$, of Eq. (2.1), which correspond to waves incident on the barrier from the left and right sides, respectively. The incoming waves are specified by e^{ik_1x} for ψ_1 and e^{-ik_2x} for ψ_2.

In terms of these wave functions the second-quantized field operator Ψ can be written as

$$\Psi=\Psi_1+\Psi_2 \ , \tag{2.5}$$

where

$$\Psi_1=\frac{1}{\sqrt{2\pi}}\int_0^\infty dk_1 \, \psi_1(k_1,x)\mathbf{a}_1(k_1)e^{-i\omega_{k_1}t} \tag{2.6}$$

and

$$\Psi_2=\frac{1}{\sqrt{2\pi}}\int_0^\infty dk_2 \, \psi_2(k_2,x)\mathbf{a}_2(k_2)e^{-i\omega_{k_2}t} \ . \tag{2.7}$$

Again, the subscripts 1 and 2 on ψ refer to particles coming at the barrier from the left and right sides, respectively. The annihilation operators $\mathbf{a}_1$ and $\mathbf{a}_2$ satisfy the usual anticommutation relations

$$[\mathbf{a}_r(k_r), \mathbf{a}_s(k_s')]_- = \delta_{rs}\delta(k_r-k_s') \ , \tag{2.8}$$

where $r,s \in \{1,2\}$.

The field operator Ψ satisfies the Schrödinger equation:

$$i\hbar\frac{\partial\Psi}{\partial t}=-\frac{\hbar^2}{2m}\frac{\partial^2\Psi}{\partial x^2}+V(x)\Psi \ . \tag{2.9}$$

The probability density operator is

$$\rho=\Psi^\dagger\Psi \ , \tag{2.10}$$

and the associated probability current operator is

$$\mathbf{J}=\frac{\hbar}{2im}\left[\Psi^\dagger\frac{\partial\Psi}{\partial x}-\frac{\partial\Psi^\dagger}{\partial x}\Psi\right] \ . \tag{2.11}$$

The operators ρ and $\mathbf{J}$ satisfy the continuity equation

$$\frac{\partial\rho}{\partial t}+\frac{\partial\mathbf{J}}{\partial x}=0 \ . \tag{2.12}$$

Similarly, associated with the momentum-density operator

$$\rho_p=-\frac{i\hbar}{2}\left[\Psi^\dagger\frac{\partial\Psi}{\partial x}-\frac{\partial\Psi^\dagger}{\partial x}\Psi\right] \tag{2.13}$$

is the momentum-current operator

$$\mathbf{J}_p=\frac{\hbar^2}{4m}\left[2\frac{\partial\Psi^\dagger}{\partial x}\frac{\partial\Psi}{\partial x}-\Psi^\dagger\frac{\partial^2\Psi}{\partial x^2}-\frac{\partial^2\Psi^\dagger}{\partial x^2}\Psi\right] \ . \tag{2.14}$$

The operators ρ_p and $\mathbf{J}_p$ are related by

$$\frac{\partial\rho_p}{\partial t}+\frac{\partial\mathbf{J}_p}{\partial x}=-\frac{\partial V(x)}{\partial x}\Psi^\dagger\Psi \ . \tag{2.15}$$

This is not generally a continuity equation, because the particle can exchange momentum with the potential when $\partial V(x)/\partial x \neq 0$.

The experimentally measured current, $\mathbf{J}_m$, is a filtered version of $\mathbf{J}$ because of parasitic reactances and instrument response times. Hence, the operator for the measured current is

$$\mathbf{J}_m(t)=\int_{-\infty}^{\infty}H(t-\tau)\mathbf{J}(\tau)d\tau \ , \tag{2.16}$$

where $H(t-\tau)$ is a causal filter function: $H(t)=0$ for $t<0$ and $\int_{-\infty}^{\infty}H^2(t)dt$ finite. In addition, it will be convenient to take $H(t)$ to be a unit response function:

$$\int_{-\infty}^{\infty}H(t)dt=1 \ . \tag{2.17}$$

From the operator (2.16) the mean tunneling current, $\langle \mathbf{J}_m \rangle$, and its variance, $(\Delta\mathbf{J}_m)^2$, can be computed. Let τ be some time interval and B be the filter-function bandwidth; then the mean, $\langle N \rangle$, and the variance, $(\Delta N)^2$, in the number of electrons N that tunnel across the barrier during the time τ are given by

$$\langle N \rangle = \langle \mathbf{J}_m \rangle \tau \tag{2.18}$$

and

$$(\Delta N)^2=\frac{\tau}{2B}(\Delta\mathbf{J}_m)^2 \ . \tag{2.19}$$

This last equation follows from the Wiener-Khintchine theorem under the assumption that τ and $1/B$ are large compared to the characteristic correlation time for $\mathbf{J}(t)$.

Let l denote the distance between the two walls of the tunneling barrier. The tunneling current is a function of l, so a measurement of N allows one to infer l. Fluctuations in the tunneling current become fluctuations in the inferred l, and the uncertainty in l is

$$\Delta l=\frac{\Delta N}{\left|\frac{\partial N}{\partial l}\right|} \ . \tag{2.20}$$

For small-amplitude motions, a mechanical system such as a tunneling probe can be represented as a collection of harmonic oscillators. Since momentum noise is transformed into position noise after one-quarter of a harmonic oscillator's period, we need also to consider the momentum noise introduced by the tunneling process. To determine how much of an incoming particle's momentum is deposited on each half of the system, we need to decompose the barrier $V(x)$ into two parts:

$$V(x)=V_1(x)+V_2(x)\ , \tag{2.21}$$

where

$$F_1=\frac{\partial V_1(x)}{\partial x} \tag{2.22}$$

and

$$F_2=\frac{\partial V_2(x)}{\partial x} \tag{2.23}$$

are the forces exerted on the electron by the left- and right-hand electrodes of the tunnel junction. We require that F_1 and F_2 go to zero for x outside of $[l_1,l_2]$. If we look to Eq. (2.15) to find the momentum transferred to the potential, we can write the momentum current into the right electrode of the tunneling probe, $\mathbf{J}_{p2}$, as

$$\mathbf{J}_{p2}=\mathbf{J}_p(l_2)+\int_{l_1}^{l_2}\frac{\partial V_2(x)}{\partial x}\Psi^\dagger\Psi\,dx\ . \tag{2.24}$$

The limits of integration are chosen to include the region where $V_2(x)$ is not constant. The first term on the right-hand side of Eq. (2.24) is the momentum current of the electrons after they have crossed the barrier. The second term accounts for the momentum delivered to the right electrode by the force it exerts on the electron.

The momentum manifests itself as a change in the tunneling current as the tunneling probe masses move. Hence, in terms of characterizing the transducer noise, the momentum current of interest is the measured momentum current

$$\mathbf{J}_{pm}(t)=\int_{-\infty}^{\infty}H(t-\tau)\mathbf{J}_{p2}(\tau)d\tau\ , \tag{2.25}$$

where H is the same filter function that appears in Eq. (2.16). The mean $\langle p\rangle$ and variance $(\Delta p)^2$ of the momentum deposited into the right-hand electrode during a time τ is thus

$$\langle p\rangle=\langle\mathbf{J}_{pm}\rangle\tau \tag{2.26}$$

and

$$(\Delta p)^2=\frac{\tau}{2B}(\Delta\mathbf{J}_{pm})^2 \tag{2.27}$$

where B is the filter bandwidth, as defined in Eq. (2.19).

We now have the basic expressions required for evaluating the position-momentum uncertainty product. In evaluating this uncertainty product it is important to keep in mind that some of the momentum fluctuations may be correlated with the tunneling current fluctuations. This correlated noise can be eliminated by standard techniques. Hence, it is the component of the momentum noise that is uncorrelated with the current noise that is of interest. Let r denote the correlation coefficient for the particle and momentum current:

$$r=\frac{\langle\frac{1}{2}(\mathbf{J}_{pm}\mathbf{J}_m+\mathbf{J}_m\mathbf{J}_{pm})\rangle-\langle\mathbf{J}_{pm}\rangle\langle\mathbf{J}_m\rangle}{\Delta\mathbf{J}_{pm}\,\Delta\mathbf{J}_m}\ . \tag{2.28}$$

The variance $(\Delta p_r)^2$ of the uncorrelated momentum noise is then

$$(\Delta p_r)^2=(1-r^2)(\Delta p)^2\ . \tag{2.29}$$

The position-momentum uncertainty product of interest is thus $\Delta p_r\,\Delta l$.

III. EXPECTATION VALUES

We now evaluate the means and variances of the particle-current and momentum-current operators for the case when the incoming electrons on both sides of the barrier satisfy Fermi-Dirac statistics. Let μ_1 and μ_2 denote the chemical potentials on the left- and right-hand sides of the barrier, respectively, and let $\beta=1/k_BT$ where k_B is Boltzmann's constant and T is the temperature. Then, the occupation functions for the left- and right-hand sides of the barrier are, respectively,

$$\rho_1(k_1)=\frac{1}{e^{-\beta[\mu_1+E(k_1)]}+1} \tag{3.1}$$

and

$$\rho_2(k_2)=\frac{1}{e^{-\beta[\mu_2+E(k_2)]}+1}\ . \tag{3.2}$$

We will need the following expectation values:

$$\langle\mathbf{a}_r^\dagger(k_r)\mathbf{a}_s(k_s)\rangle=\delta_{rs}\delta(k_r-k_s)\rho_r(k_r) \tag{3.3}$$

and

$$\begin{aligned}\langle\mathbf{a}_r^\dagger(k_r)\mathbf{a}_s^\dagger(k_s)\mathbf{a}_u(k_u)\mathbf{a}_v(k_{bv})\rangle&\\ =[\delta_{rv}\delta_{su}\delta(k_r-k_v)\delta(k_s-k_u)&\\ -\delta_{ru}\delta_{sv}\delta(k_r-k_u)\delta(k_s-k_v)]\rho_r(k_r)\rho_s(k_s)\ ,&\end{aligned} \tag{3.4}$$

where r, s, u, and v are elements of $\{1,2\}$.

Using Eqs. (2.5)–(2.7) for the form of Ψ, and Eqs. (2.11) and (2.16) for the definition of $\mathbf{J}_m$, one can write the measured momentum current in the following form:

$$\begin{aligned}\mathbf{J}_m=\frac{1}{2\pi}\sum_{r,s}\int_0^\infty dk_r\int_0^\infty dk_s'\,A_{rs}(k_r,k_s')&\\ \times h(\omega_{ks}'-\omega_{kr})e^{i(\omega_{kr}-\omega_{ks}')t}&\\ \times\mathbf{a}_r^\dagger(k_r)\mathbf{a}_s(k_s')\ ,&\end{aligned} \tag{3.5}$$

where

$$A_{rs}(k_r,k_s')=\frac{\hbar}{2im}\left[\psi_r^*(k_r,x)\frac{\partial\psi_s(k_s',x)}{\partial x}-\frac{\partial\psi_r^*(k_r,x)}{\partial x}\psi_s(k_s',x)\right]\ . \tag{3.6}$$

The function $h(\omega)$ is the Fourier transform of the filter function $H(t)$,

$$h(\omega)=\int_{-\infty}^{\infty}H(t)e^{i\omega t}dt\ . \tag{3.7}$$

Since $H(t)$ is real, $h(\omega)$ satisfies the relation

$$h(\omega)=h^*(-\omega) \tag{3.8}$$

and, since $H(t)$ is a unit response function, one also has

$$h(0)=1 \ . \tag{3.9}$$

Similarly, the momentum-current operator $\mathbf{J}_{pm}$ has the form

$$\mathbf{J}_{pm}=\frac{1}{2\pi}\sum_{r,s}\int_0^\infty dk_r\int_0^\infty dk_s' \, B_{rs}(k_r,k_s')h(\omega_{k's}-\omega_{kr})e^{i(\omega_{kr}-\omega_{k's})t}\mathbf{a}_r^\dagger(k_r)\mathbf{a}_s(k_s') \ , \tag{3.10}$$

where

$$B_{rs}(k_r,k_s')=\left[\frac{\hbar^2}{4m}\left[2\frac{\partial\psi_r^*(k_r,x)}{\partial x}\frac{\partial\psi_s(k_s',x)}{\partial x}-\psi_r^*(k_r,x)\frac{\partial^2\psi_s(k_s',x)}{\partial x^2}-\frac{\partial^2\psi_r^*(k_r,x)}{\partial x^2}\psi_s(k_s',x)\right]_{l_2}\right.$$
$$\left.+\int_{-\infty}^{\infty}\frac{\partial V_2(x)}{\partial x}\psi_r^*(k_r,x)\psi_s(k_s',x)dx\right] \ . \tag{3.11}$$

If we take expectation values of the particle current and momentum current, Eq. (3.3) can be used to collapse one of the two integrals appearing in the equations for $\mathbf{J}_m$ and $\mathbf{J}_{pm}$ [Eqs. (3.5) and (3.10)]. The corresponding expectation values are

$$\langle\mathbf{J}_m\rangle=\frac{1}{2\pi}\sum_{r=1}^{2}\int_0^\infty dk_r \, A_{rr}(k_r,k_r)\rho_r(k_r) \tag{3.12}$$

and

$$\langle\mathbf{J}_{pm}\rangle=\frac{1}{2\pi}\sum_{r=1}^{2}\int_0^\infty dk_r \, B_{rr}(k_r,k_r)\rho_r(k_r) \ . \tag{3.13}$$

Similarly, we use Eq. (3.4) to collapse the integrals for the variances and correlation. We find

$$\langle\mathbf{J}_m\mathbf{J}_{pm}\rangle-\langle\mathbf{J}_m\rangle\langle\mathbf{J}_{pm}\rangle=\left[\frac{1}{2\pi}\right]^2\sum_{r,s}\int_0^\infty dk_r\int_0^\infty dk_s' \, A_{rs}(k_r,k_s')B_{sr}(k_s',k_r)\rho_r(k_r)[1-\rho_s(k_s')]\,|h(\omega_{ks'}-\omega_{kr})|^2 \ . \tag{3.14}$$

The expressions for $(\Delta\mathbf{J}_m)^2$ and $(\Delta\mathbf{J}_{pm})^2$ have a form similar to Eq. (3.14), but with $A_{rs}(k_r,k_s')B_{sr}(k_s',k_r)$ replaced by $A_{rs}(k_r,k_s')A_{sr}(k_s',k_r)$ and $B_{rs}(k_r,k_s')B_{sr}(k_s',k_r)$, respectively.

We can simplify these expectation values further in a practical experimental situation. Since the bandwidth over which one might measure these small currents is less than 1 GHz, the energy scale $E=\hbar\omega$ over which $h(\omega)$ is nonzero is small compared to energy scales over which A_{rs}, B_{rs}, ρ_r, and ρ_s vary. Hence, to a good approximation, Eq. (3.14) reduces to

$$\langle\mathbf{J}_m\mathbf{J}_{pm}\rangle-\langle\mathbf{J}_m\rangle\langle\mathbf{J}_{pm}\rangle=\left[\frac{1}{2\pi}\right]^2\sum_{r,s}\int_0^\infty dk_r \, A_{rs}(k_r,k_s)B_{sr}(k_s,k_r)\rho_r(k_r)[1-\rho_s(k_s)]\int_0^\infty dk_s' \, |h(\omega_{ks'}-\omega_{kr})|^2 \ , \tag{3.15}$$

where k_s and k_r are given by Eq. (2.4).

Since the particle dispersion relation outside the barrier is

$$\hbar\omega_{k's}=\frac{\hbar^2k_s'^2}{2m}+V_s \ , \tag{3.16}$$

one has

$$dk_s'=\frac{m}{\hbar k_s'}d\omega_{k's} \ , \tag{3.17}$$

and the dk_s' integral of the correlation function [Eq. (3.15)] can be approximated as

$$\int_0^\infty dk_s' \, |h(\omega_{k's}-\omega_{kr})|^2=\frac{m}{\hbar k_s}4\pi B \ , \tag{3.18}$$

where B is the filter-function bandwidth

$$B=\frac{1}{2\pi}\int_{-\infty}^{\infty}d\omega\,|h(\omega)|^2 \ . \tag{3.19}$$

So, one finally obtains the following expression for the cross-correlation between the current and momentum current:

$$\langle\mathbf{J}_m\mathbf{J}_{pm}\rangle-\langle\mathbf{J}_m\rangle\langle\mathbf{J}_{pm}\rangle=\frac{B}{2\pi}\sum_{r,s}\int_0^\infty dk_r\frac{m}{\hbar k_s}A_{rs}(k_r,k_s)B_{sr}(k_s,k_r)\times\rho_r(k_r)[1-\rho_s(k_s)] \ . \tag{3.20}$$

Similarly, the current variance is given by

$$(\Delta\mathbf{J}_m)^2=\frac{B}{2\pi}\sum_{r,s}\int_0^\infty dk_r\frac{m}{\hbar k_s}A_{rs}(k_r,k_s)A_{sr}(k_s,k_r)\times\rho_r(k_r)[1-\rho_s(k_s)] \ , \tag{3.21}$$

and the momentum-current variance is given by

$$(\Delta \mathbf{J}_{pm})^2=\frac{B}{2\pi}\sum_{r,s}\int_0^\infty dk_r\frac{m}{\hbar k_s}B_{rs}(k_r,k_s)B_{sr}(k_s,k_r)$$
$$\times\rho_r(k_r)[1-\rho_s(k_s)]\ . \tag{3.22}$$

Before applying this formalism to specific examples, we make one more approximation, the zero-temperature approximation. The occupation functions $\rho_r(k_r)$, defined in Eqs. (3.1) and (3.2), then become Heaviside unit-step functions

$$\rho_r(k_r)=\Theta(k_{Fr}-k_r)\ , \tag{3.23}$$

where

$$\Theta(x)=\begin{cases}1 & \text{for } x>0\ ,\\ \frac{1}{2} & \text{for } x=0\ ,\\ 0 & \text{for } x<0\ ,\end{cases} \tag{3.24}$$

and k_{Fr} is the Fermi momentum for the rth electrode ($r\in\{1,2\}$) of the tunneling probe. Let us take the Fermi energy to be higher in electrode 1 than in electrode 2, then all the $\rho_r(k_r)[1-\rho_s(k_s)]$ in the variances and correlations [Eqs. (3.20)–(3.22)] are zero except when $r=1$ and $s=2$. Equations (3.20)–(3.22) thus reduce to

$$\langle \mathbf{J}_m\mathbf{J}_{pm}\rangle-\langle \mathbf{J}_m\rangle\langle \mathbf{J}_{pm}\rangle$$
$$=\frac{B}{2\pi}\int_{k_{L1}}^{k_{F1}}dk_1\frac{m}{\hbar k_2}A_{12}(k_1,k_2)B_{21}(k_2,k_1)\ , \tag{3.25}$$

$$(\Delta \mathbf{J}_m)^2=\frac{B}{2\pi}\int_{k_{L1}}^{k_{F1}}dk_1\frac{m}{\hbar k_2}A_{12}(k_1,k_2)A_{21}(k_2,k_1)\ , \tag{3.26}$$

and

$$(\Delta \mathbf{J}_{pm})^2=\frac{B}{2\pi}\int_{k_{L1}}^{k_{F1}}dk_1\frac{m}{\hbar k_2}B_{12}(k_1,k_2)B_{21}(k_2,k_1)\ . \tag{3.27}$$

The lower limit of integration, k_{L1}, is determined by the Fermi energy E_{F2} on the right-hand side of the barrier, i.e.,

$$E_{F2}=\frac{\hbar^2k_{L1}^2}{2m}+V_1\ . \tag{3.28}$$

From Eqs. (3.25)–(3.27) one sees that states which are filled or empty on both sides of the barrier do not contribute to fluctuations. Going back to the definitions of $\mathbf{J}_m$ and $\mathbf{J}_{pm}$ [Eqs. (3.5) and (3.10)], one sees that the noise arises from expressions containing the products $\mathbf{a}_1^\dagger(k_1)\mathbf{a}_2(k_2')$ and $\mathbf{a}_2^\dagger(k_2)\mathbf{a}_1(k_1')$. The noise can thus be regarded as resulting from the interference of vacuum fluctuations coming in from the right-hand side of the barrier with the electrons that tunnel through the left-hand side of the barrier.

IV. SHOT NOISE

In this section we make use of the properties of ψ_1 and ψ_2 outside the barrier region to further simplify the expressions for $\langle \mathbf{J}_m\rangle$ and $(\Delta \mathbf{J}_m)^2$. The usual shot-noise formulas can then readily be derived. Let $A_1e^{ik_1x}$ and $A_2e^{-ik_2x}$ be plane waves approaching the barrier from the left and from the right, and let $B_1e^{-ik_1x}$ and $B_2e^{+ik_2x}$ be the plane waves leaving the barrier on the right and left, respectively.

The amplitudes B_1 and B_2 are related to A_1 and A_2 via the scattering matrix M:

$$\begin{bmatrix}B_1\\B_2\end{bmatrix}=\begin{bmatrix}M_{11}&M_{12}\\M_{21}&M_{22}\end{bmatrix}\begin{bmatrix}A_1\\A_2\end{bmatrix}\ . \tag{4.1}$$

In terms of the M_{ij}, the wave functions $\psi_1(x)$ and $\psi_2(x)$ are

$$\psi_1(k_1,x)=\begin{cases}e^{ik_1x}+M_{11}e^{-ik_1x} & \text{for } x<l_1\ ,\\ M_{21}e^{ik_2k} & \text{for } x>l_2\ ,\end{cases} \tag{4.2}$$

and

$$\psi_2(k_2,x)=\begin{cases}M_{12}e^{ik_1x} & \text{for } x<l_1\ ,\\ e^{-ik_2x}+M_{22}e^{ik_2x} & \text{for } x>l_2\ .\end{cases} \tag{4.3}$$

The M_{ij} are not independent; they are constrained because the scattering of a particle off the barrier is elastic, and we assume particles are neither created nor destroyed.

The constraints on the M_{ij} are most easily derived as follows: Let N_D be the difference in the number of electrons that eventually arrive at $+\infty$ and $-\infty$:

$$N_D=\int_{-\infty}^{\infty}\mathbf{J}_m(x)dt\ . \tag{4.4}$$

Clearly this difference does not depend on the position x at which one chooses to evaluate N_D. Substituting $\mathbf{J}_m$ [Eq. (3.5)] into Eq. (4.4), one obtains

$$N_D=\sum_{r,s}\int_0^\infty dk_r\frac{m}{\hbar k_s}A_{rs}(k_r,k_s)\mathbf{a}_r^\dagger(k_r)\mathbf{a}_s(k_s)\ , \tag{4.5}$$

where

$$k_s=\left[k_r^2+\frac{2m}{\hbar^2}(V_s-V_r)\right]^{1/2}\ . \tag{4.6}$$

It follows that $A_{rs}(k_r,k_s)$ must be independent of position. Hence, evaluating $A_{rs}(k_r,k_s)$ on both sides of the barrier using its definition [Eq. (3.6)] and the wave function outside the barrier, Eqs. (4.2) and (4.3), one finds that the matrix

$$\begin{bmatrix}M_{11}&(k_1/k_2)^{1/2}M_{12}\\(k_2/k_1)^{1/2}M_{21}&M_{22}\end{bmatrix} \tag{4.7}$$

is unitary.

Useful relations that easily follow from the unitarity of the matrix equation (4.7) are

$$|M_{11}|^2=|M_{22}|^2\ , \tag{4.8}$$

$$\frac{k_2}{k_1}|M_{21}|^2=\frac{k_1}{k_2}|M_{12}|^2 , \tag{4.9}$$

and

$$1-|M_{11}|^2=\frac{k_2}{k_1}|M_{21}|^2 . \tag{4.10}$$

The A_{rs} evaluated for $x>l_2$ are

$$A_{11}(k_1,k_2)=\frac{\hbar k_2}{m}|M_{21}|^2 , \tag{4.11}$$

$$A_{22}(k_2,k_2)=-\frac{\hbar k_2}{m}(1-|M_{22}|^2) , \tag{4.12}$$

$$A_{12}(k_1,k_2)=\frac{\hbar k_2}{m}M_{21}^*M_{22} , \tag{4.13}$$

and

$$A_{21}(k_1,k_2)=\frac{\hbar k_2}{m}M_{22}^*M_{21} . \tag{4.14}$$

Using Eqs. (4.8)–(4.12), the expression for the mean current [Eq. (3.12)] can be put into the form

$$\langle \mathbf{J}_m \rangle=\frac{1}{2\pi}\int_0^\infty dk_2\frac{\hbar k_1}{m}|M_{12}|^2[\rho_1(k_1)-\rho_2(k_2)] . \tag{4.15}$$

Again, taking the zero-temperature limit, this can be expressed as

$$\langle \mathbf{J}_m \rangle=\frac{1}{2\pi}\int_{k_{L1}}^{k_{F1}}dk_1\frac{\hbar k_2}{m}|M_{21}|^2 . \tag{4.16}$$

A similar substitution [Eqs. (4.13) and (4.14) into Eq. (3.26)] yields the variance of $\mathbf{J}_m$:

$$(\Delta\mathbf{J}_m)^2=\frac{B}{\pi}\int_{k_{L1}}^{k_{F1}}dk_1\frac{\hbar k_2}{m}|M_{21}(E)|^2|M_{22}(E)|^2 . \tag{4.17}$$

When the transmission probability through the barrier is small, which is generally the case in scanning-tunneling microscopy, the reflection coefficient $|M_{22}|^2$ is very nearly unity and one has

$$(\Delta\mathbf{J}_m)^2=\frac{B}{\pi}\int_{k_{L1}}^{k_{F1}}dk_1\frac{\hbar k_2}{m}|M_{21}(E)|^2 . \tag{4.18}$$

If we compare this equation with that for the mean current, Eq. (4.16), we obtain the usual shot-noise formula

$$(\Delta\mathbf{J}_m)^2=2B\langle \mathbf{J}_m \rangle . \tag{4.19}$$

Using the relations between $\mathbf{J}$ and N [Eqs. (2.18) and (2.19)], one finds that the variance is equal to the mean for the number of particles crossing the barrier in a time interval τ:

$$(\Delta N)^2=\langle N \rangle . \tag{4.20}$$

V. THE RECTANGULAR BARRIER

In this section the position and momentum uncertainties for a rectangular barrier are evaluated. We show that for such a barrier an uncertainty product of $\hbar/2$ can be realized. This is the minimum dispersion in position and momentum allowed by quantum mechanics. The barrier is taken to have the form

$$V(x)=\begin{cases} V & \text{for } x<l_1 , \\ V_b & \text{for } l_1<x<l_2 , \\ V & \text{for } l_2<x . \end{cases} \tag{5.1}$$

Note that Eq. (2.2) specializes to $V_1=V_2=V$. Such a potential can be expected to give a reasonably good description of low-voltage tunneling between electrodes made of the same metal.

When the energy E of the tunneling electron is less than V_b, the wave functions in the region $l_1<x<l_2$ have the forms

$$\begin{aligned} \psi_1&=R_{11}e^{-k_bx}+R_{12}e^{k_bx} , \\ \psi_2&=R_{21}e^{-k_bx}+R_{22}e^{k_bx} , \end{aligned} \tag{5.2}$$

where

$$k_b=\left[\frac{2m}{\hbar^2}(V_b-E)\right]^{1/2} . \tag{5.3}$$

If we match ψ and ψ' at l_1 and l_2, using Eqs. (4.2), (4.3), and (5.2), we obtain

$$M_{11}=i(k^2+k_b^2)\sinh[k_b(l_1-l_2)]e^{-i2kl_1}/D(k) , \tag{5.4}$$

$$M_{12}=M_{21}=2kk_be^{ik(l_1-l_2)}/D(k) , \tag{5.5}$$

and

$$M_{22}=i(k^2+k_b^2)\sinh[k_b(l_1-l_2)]e^{-i2kl_2}/D(k) , \tag{5.6}$$

where

$$\begin{aligned} D(k)=&2kk_b\cosh[k_b(l_1-l_2)] \\ &-i(k_b^2-k^2)\sinh[k_b(l_1-l_2)] . \end{aligned} \tag{5.7}$$

In writing Eqs. (5.4)–(5.7) we have used the fact that $V_1=V_2=V$, which implies $k_1=k_2=k$.

Under low-bias voltage conditions the difference Δk in the Fermi momenta on the left- and right-hand sides of the barrier will be small compared to the scale on which M_{ij} vary. Hence, the integrals for the expectation values of the current [Eqs. (4.16) and (4.17)] become

$$\langle \mathbf{J}_m \rangle=\frac{1}{2\pi}\frac{\hbar k}{m}|M_{21}|^2\Delta k \tag{5.8}$$

and

$$\langle(\Delta\mathbf{J}_m)^2\rangle=\frac{B}{\pi}\frac{\hbar k}{m}|M_{21}|^2|M_{22}|^2\Delta k . \tag{5.9}$$

Using Eqs. (2.18) and (2.19) to connect $\mathbf{J}$ and N, one obtains

$$\langle N \rangle=|M_{21}|^2 n \tag{5.10}$$

and

$$(\Delta N)^2=|M_{12}|^2|M_{22}|^2 n , \tag{5.11}$$

where

$$n=\frac{\hbar k\,\Delta k\,\tau}{2\pi m} \tag{5.12}$$

can be thought of as the number of electrons attempting to tunnel across the barrier in the measurement time τ.

If we insert the expressions for $\mathbf{M}$ [Eqs. (5.4)–(5.6)] into Eqs. (5.10)–(5.12), we obtain

$$\langle N\rangle=\frac{4k^2k_b^2}{|D(k)|^2}n \tag{5.13}$$

and, using Eq. (2.20) to deduce the inferred position noise from ΔN,

$$\Delta l=\frac{|D(k)|^2}{4n^{1/2}kk_b^2(k_b^2+k^2)\cosh[k_b(l_1-l_2)]}\ . \tag{5.14}$$

For $k_b(l_1-l_2)\gg 1$, these expressions simplify to

$$\langle N\rangle=16k^2k_b^2e^{-2k_b(l_2-l_1)} \tag{5.15}$$

and

$$\Delta l=\frac{(k_b^2+k^2)e^{k_b(l_2-l_1)}}{8n^{1/2}kk_b^2}\ . \tag{5.16}$$

From Eq. (5.15) one sees that the mean number of particles crossing the barrier decreases exponentially with the barrier width l. From Eq. (5.16) one sees that uncertainty in the inferred barrier width increases exponentially in l, but decreases as the square root of the number of particles that have crossed the barrier.

For the square-well potential, as defined in Eq. (5.1),

$$\frac{\partial V_2(x)}{\partial x}=-(V_b-V)\delta(x-l_2)\ . \tag{5.17}$$

We integrate Eq. (2.15) from $x_1=l_2-\epsilon$ to $x_2=l_2+\epsilon$ and take the limit $\epsilon\to 0$ to obtain

$$\mathbf{J}_p(l_2^-)=\mathbf{J}_p(l_2^+)-(V_b-V)\Psi^\dagger(l_2)\Psi(l_2)\ . \tag{5.18}$$

The above equation may be compared with the expression for the momentum transferred into the right electrode [Eq. (2.24)] to find that

$$\mathbf{J}_{p2}=\mathbf{J}_p(l_2^-)\ , \tag{5.19}$$

that is, $\mathbf{J}_{p2}$ is the momentum current through the barrier.

We are now in a position to evaluate the B_{rs} which appear in the expression for $\mathbf{J}_{pm}$ [Eq. (3.10)]. We can substitute expressions for the wave functions outside the barrier [Eqs. (4.2) and (4.3)] into Eq. (3.11), which defines the B_{rs}, to get

$$B_{11}(k,k)=\frac{\hbar^2}{2m}(k^2-k_b^2)|M_{21}|^2\ , \tag{5.20}$$

$$\begin{aligned}B_{12}(k,k)&=B_{21}^*(k,k)\\&=-\frac{\hbar^2}{2m}(k^2+k_b^2)M_{21}^*e^{-2ikl_2}\\&\quad+\frac{\hbar^2}{2m}(k^2-k_b^2)M_{21}^*M_{22}\ ,\end{aligned} \tag{5.21}$$

$$B_{22}(k,k)=\frac{\hbar^2}{2m}(k^2-k_b^2)|M_{21}|^2\ . \tag{5.22}$$

In obtaining Eq. (5.22) use was made of the relationship

$$(k^2-k_b^2)|M_{22}|^2=(k^2+k_b^2)\mathrm{Re}(M_{22}e^{i2kl_2})\ , \tag{5.23}$$

which can be derived from Eqs. (5.6) and (4.10).

The expressions for the A_{rs} [Eqs. (4.11)–(4.14)], the B_{rs} [Eqs. (5.20)–(5.22)], and M [Eqs. (5.4)–(5.7)] can now be substituted into Eq. (3.13), the general expressions for $\langle\mathbf{J}_{pm}\rangle$, to obtain the mean momentum current flowing across the barrier. The mean momentum transferred is

$$\langle\mathbf{J}_{pm}\rangle=\frac{1}{2\pi}\int_0^\infty dk\frac{\hbar^2}{2m}(k^2-k_b^2)|M_{21}|^2[\rho_1(k)+\rho_2(k)]\ . \tag{5.24}$$

Similarly, one also finds that the real part of the cross-correlation equation (3.25) between the particle current and momentum current is zero:

$$\mathrm{Re}(\langle\mathbf{J}_m\mathbf{J}_{pm}\rangle-\langle\mathbf{J}_m\rangle\langle\mathbf{J}_{pm}\rangle)=0\ . \tag{5.25}$$

Hence, the correlation coefficient r [Eq. (2.28)] is zero. Thus, for the square barrier potential, Eq. (5.1), the tunneling current and the momentum current are uncorrelated. Again, we obtain the variance of $\mathbf{J}_{pm}$ by substituting Eq. (5.21) into Eq. (3.27):

$$\begin{aligned}(\Delta\mathbf{J}_{pm})^2=\frac{B}{\pi}\frac{m\,\Delta k}{\hbar k}\left[\frac{\hbar^2}{2m}\right]^2|M_{21}|^2\\\times[(k^2+k_b^2)^2-(k^2-k_b^2)^2|M_{22}|^2]\ .\end{aligned} \tag{5.26}$$

We next use Eqs. (5.5) and (5.6) to supply M_{21} and M_{22}, and Eq. (2.27) to relate the momentum transfer to the momentum current. The momentum uncertainty is found to be

$$\Delta p\frac{2n^{1/2}\hbar kk_b^2(k^2+k_b^2)}{|D(k)|^2}\cosh[k_b(l_1-l_2)]\ . \tag{5.27}$$

The position-momentum uncertainty product can now be evaluated by multiplying Eqs. (5.14) and (5.27). One obtains

$$\Delta l\,\Delta p=\hbar/2\ . \tag{5.28}$$

This is the minimum position-momentum uncertainty product allowed by quantum mechanics. A vacuum tunneling probe can thus perform position measurements with the smallest allowed dispersion in p.

VI. TUNNELING IN THE PRESENCE OF AN ELECTRIC FIELD

In this section we evaluate the position-momentum uncertainty product for the more realistic case when a nonzero electric field is present between the two electrodes. It is shown that for realistic barrier parameters the uncertainty product differs from $\hbar/2$ by less than 1%.

The potential is depected in Fig. 2 and is given by

$$V(x)=\begin{cases} V_1 \text{ for } x<l_1 , \\ \dfrac{V_{b2}-V_{b1}}{l_2-l_1}(x-l_1)+V_{b1} \text{ for } l_1<x<l_2 , \\ V_2 \text{ for } l_2<x . \end{cases} \quad (6.1)$$

The slope in the potential between l_1 and l_2 is due to the electric field appearing between the two electrodes. Since the electrostatic attraction of the electron towards one electrode is equal to the electrostatic repulsion from the other, the interaction of the electron with the right electrode, $V_2(x)$, can be written as

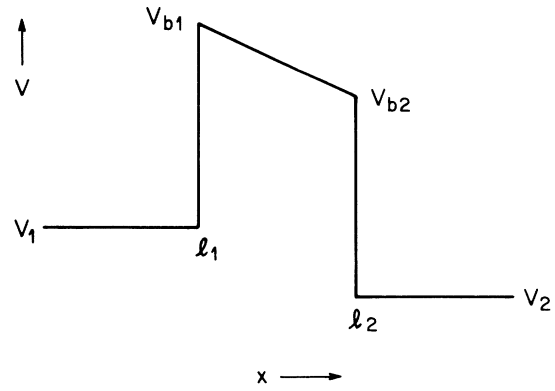

FIG. 2. A rectangular barrier in the presence of an applied voltage.

$$V_2(x)=\begin{cases} \frac{1}{2}(V_{b2}+V_{b1}) \text{ for } x<l_1 , \\ \dfrac{1}{2}\left[\dfrac{V_{b2}-V_{b1}}{l_2-l_1}\right](x-l_1)+\frac{1}{2}(V_{b2}+V_{b1}) \text{ for } l_1<x<l_2 , \\ V_2 \text{ for } l_2<x . \end{cases} \quad (6.2)$$

$V_2(x)$ is defined in Eqs. (2.21)–(2.23). The B_{rs}, Eq. (3.11), can now be written in the form

$$B_{rs}(k_r,k_s')=C_{rs}(k_r,k_s')+\frac{1}{2}\left[\frac{V_{b2}-V_{b1}}{l_2-l_1}\right]\int_{l_1}^{l_2}\psi_r^*(k_r,x)\psi_s(k_s',x)dx , \quad (6.3)$$

where

$$C_{rs}(k_r,k_s')=\frac{\hbar^2}{4m}\left[2\frac{\partial\psi_r^*(k_r,x)}{\partial x}\frac{\partial\psi_s(k_s',x)}{\partial x}-\psi_r^*(k_r,x)\frac{\partial^2\psi_s(k_s',x)}{\partial x^2}-\frac{\partial^2\psi_r^*(k_r,x)}{\partial x^2}\psi_s(k_s',x)\right]_{x=l_2^+} -(V_{b2}-V_2)\psi_r^*(k_r,l_2)\psi_s(k_s',l_2) . \quad (6.4)$$

Using the form of the wave function outside the barrier [Eqs. (4.2) and (4.3)], the C_{rs} can be expressed in terms of the M_{ij}. In particular, one obtains

$$C_{11}(k_1,k_1)=\left[\frac{\hbar^2k_b^2}{2m}+V_2-V_{b2}\right]|M_{21}(E)|^2 , \quad (6.5)$$

$$C_{12}(k_1,k_2)=C_{21}^*(k_2,k_1) =\left[\frac{\hbar^2k_2^2}{m}+V_2-V_{b2}\right]M_{21}^*(E)M_{22}(E) +(V_2-V_{b2})M_{21}^*(E)e^{-i2k_2l_2} , \quad (6.6)$$

and

$$C_{22}(k_2,k_2)=\left[\frac{\hbar^2k_2^2}{m}+V_2-V_{b2}\right][1+|M_{22}(E)|^2] +2(V_2-V_{b2})\mathrm{Re}[M_{22}(E)e^{i2k_2l_2}] . \quad (6.7)$$

The zero-temperature variances and cross-correlation for the particle current and momentum current can now be obtained from Eqs. (3.25)–(3.27), provided one knows the scattering matrix elements $M_{ij}(E)$ and the integral appearing in Eq. (6.3). These we evaluated numerically. The calculation was done by numerically integrating the equation

$$\frac{dy^2}{dx^2}=-2k\frac{dy}{dx}+\left[\frac{2m[E-V(x)]}{\hbar^2}-k^2\right]y , \quad (6.8)$$

which has $y=\psi e^{-kx}$ as its solution, where ψ is the wave function in the Schrödinger equation (2.1). An integration across the barrier in each direction yields the information necessary to calculate the scattering matrix. Additionally, y was expanded in an (8–16)-term cosine Fourier series inside the barrier, and the series expansion was used to evaluate

$$\int_{l_1}^{l_2}\psi_r^*\psi_s\,dx$$

for use in Eq. (6.3).

The parameters used in the analysis are those depicted in Fig. 3. A spacing of 5 Å was chosen between the barrier walls. The potential difference as one crosses from the interior of an electrode to the vacuum space is 5 eV. The Fermi energy in each electrode is taken to be 1 eV. The bias voltage across the electrodes was varied from 0 to 4.0 V. The results of the uncertainty-product calculation are displayed in Fig. 4(a). Note that over the range

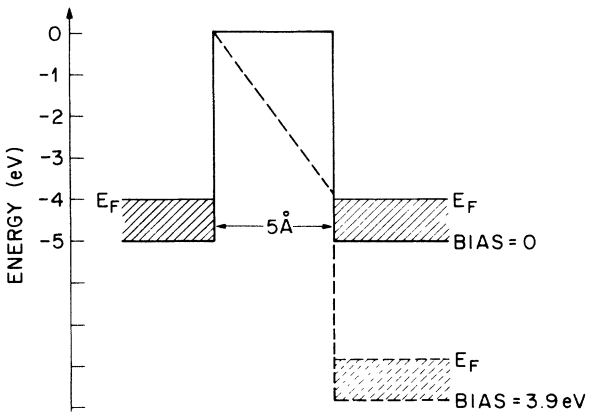

FIG. 3. This figure depicts the parameters used in the numerical calculations of the uncertainty product (Fig. 4). E_F denotes the Fermi energy.

of bias voltages applied, the uncertainty product differs from $\hbar/2$ by less than 1%. Since there is generally some correlation between the momentum current and the particle current, Eq. (2.29) was used to determine the part of the momentum noise uncorrelated with the tunneling current. Figure 4(b) displays the correlation coefficient. Although it is nonzero, it is small compared with unity.

The results described here were obtained by integrating over the Fermi sea. The results are not appreciably different from those that would have been obtained from the tunneling of a monoenergetic beam of particles at the Fermi energy. This results from the fact that the probability of tunneling rapidly increases as the electron energy increases. Energy levels near the Fermi energy thus contribute most to the tunneling current.

The numerical results presented here indicate that tunneling probes used as position transducers could come close to optimum performance even with a sizable bias voltage across the electrodes.

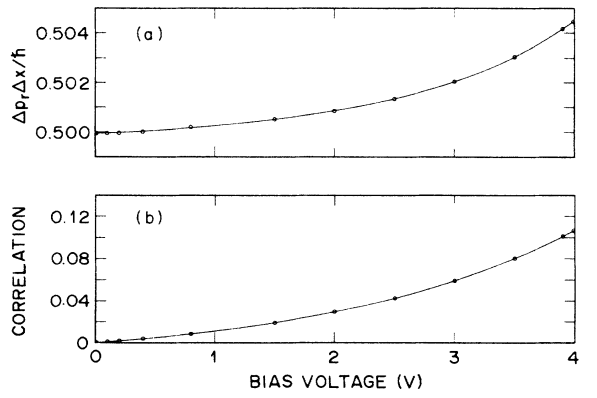

FIG. 4. (a) The position-momentum uncertainty product and (b) the correlation coefficient for the particle current and momentum current evaluated for the potential of Fig. 3. Note that the uncertainty product differs from $\hbar/2$ by less than 1% even when the bias voltage is as high as 4 V.

VII. TUNNELING THROUGH AN ATOM

The forces that result from the exchange of electrons across a barrier can be either attractive or repulsive. These covalent-bonding forces can be detected by measuring the momentum imparted to one of the electrodes. To determine the kind of information available if one measures p, tunneling through a square-well barrier with an atom attached to one wall will be evaluated here. The atom is modeled as a rectangular well within the barrier. The potential is depicted in Fig. 5 and is given by

$$V(x)=\begin{cases} V_a & \text{for } x<l_1\ , \\ V_b & \text{for } l_1<x<l_2\ , \\ V_c & \text{for } l_2<x<l_3\ , \\ V_d & \text{for } l_3<x<l_4\ , \\ V_e & \text{for } l<x\ . \end{cases} \tag{7.1}$$

We will consider the case when the energy E of the tunneling electrons satisfies $V_a<E<V_b$. An energy eigenstate then has the general form

$$\psi=\begin{cases} a_1e^{ik_ax}+a_2e^{-ik_ax} & \text{for } x<l_1\ , \\ b_1e^{-k_bx}+b_2e^{k_bx} & \text{for } l_1<x<l_2\ , \\ c_1e^{ik_cx}+c_2e^{-ik_cx} & \text{for } l_2<x<l_3\ , \\ d_1e^{-k_dx}+d_2e^{k_dx} & \text{for } l_3<x<l_4\ , \\ e_1e^{ik_ex}+e_2e^{-ik_ex} & \text{for } l_4<x\ . \end{cases} \tag{7.2}$$

Matching the wave function and its first derivative at the boundaries, one obtains transfer matrices relating the amplitudes at the boundaries. For example, at $x=l_1$ one obtains

$$\begin{bmatrix} a_1 \\ a_2 \end{bmatrix}=\begin{bmatrix} T^a_{11} & T^a_{12} \\ T^a_{21} & T^a_{22} \end{bmatrix}\begin{bmatrix} b_1 \\ b_2 \end{bmatrix}, \tag{7.3}$$

where

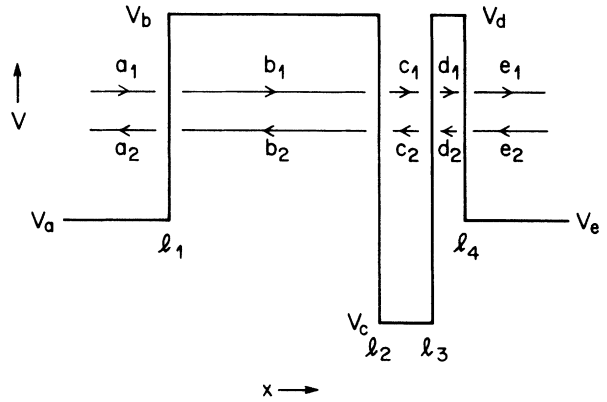

FIG. 5. A rectangular barrier with a square-well atom.

$$T_{11}^{a}=\frac{1}{2}\left[1-\frac{k_b}{ik_a}\right]e^{-ik_a l_1}e^{-k_b l_1}, \tag{7.4}$$

$$T_{12}^{a}=\frac{1}{2}\left[1-\frac{k_b}{ik_a}\right]e^{-ik_a l_1}e^{k_b l_1}, \tag{7.5}$$

$$T_{21}^{a}=\frac{1}{2}\left[1+\frac{k_b}{ik_a}\right]e^{ik_a l_1}e^{-k_b l_1}, \tag{7.6}$$

and

$$T_{22}^{a}=\frac{1}{2}\left[1-\frac{k_b}{ik_a}\right]e^{ik_a l_1}e^{k_b l_1}. \tag{7.7}$$

At $x=l_2$ one obtains

$$\begin{bmatrix} b_1 \\ b_2 \end{bmatrix}=\begin{bmatrix} T_{11}^{b} & T_{12}^{b} \\ T_{21}^{b} & T_{22}^{b} \end{bmatrix}\begin{bmatrix} c_1 \\ c_2 \end{bmatrix}, \tag{7.8}$$

where

$$T_{11}^{b}=\frac{1}{2}\left[1-\frac{ik_c}{k_b}\right]e^{k_b l_2}e^{ik_c l_2}, \tag{7.9}$$

$$T_{12}^{b}=\frac{1}{2}\left[1+\frac{ik_c}{k_b}\right]e^{k_b l_2}e^{-ik_c l_2}, \tag{7.10}$$

$$T_{21}^{b}=\frac{1}{2}\left[1+\frac{ik_c}{k_b}\right]e^{-k_b l_2}e^{ik_c l_2}, \tag{7.11}$$

and

$$T_{22}^{b}=\frac{1}{2}\left[1-\frac{ik_c}{k_b}\right]e^{-k_b l_2}e^{-ik_c l_2}. \tag{7.12}$$

One has expressions similar to Eqs. (7.3)–(7.7) or Eqs. (7.8)–(7.12) at the remaining boundaries l_3 and l_4. The overall transfer matrix relating e_1 and e_2 to a_1 and a_2 is obtained by multiplying these transfer matrices together:

$$\begin{bmatrix} T_{11} & T_{12} \\ T_{21} & T_{22} \end{bmatrix}=\begin{bmatrix} T_{11}^{a} & T_{12}^{a} \\ T_{21}^{a} & T_{22}^{a} \end{bmatrix}\begin{bmatrix} T_{11}^{b} & T_{12}^{b} \\ T_{21}^{b} & T_{22}^{b} \end{bmatrix}\times\begin{bmatrix} T_{11}^{c} & T_{12}^{c} \\ T_{21}^{c} & T_{22}^{c} \end{bmatrix}\begin{bmatrix} T_{11}^{d} & T_{12}^{d} \\ T_{21}^{2} & T_{22}^{d} \end{bmatrix}. \tag{7.13}$$

The scattering matrix M relating the incoming waves a_1 and e_2 to the outgoing waves a_2 and e_1,

$$\begin{bmatrix} a_2 \\ e_1 \end{bmatrix}=\begin{bmatrix} M_{11} & M_{12} \\ M_{21} & M_{22} \end{bmatrix}\begin{bmatrix} a_1 \\ e_2 \end{bmatrix}, \tag{7.14}$$

is obtained from the transfer matrix via

$$M_{11}=\frac{T_{21}}{T_{11}}, \tag{7.15}$$

$$M_{12}=T_{22}-\frac{T_{12}T_{21}}{T_{11}}, \tag{7.16}$$

$$M_{21}=\frac{1}{T_{11}}, \tag{7.17}$$

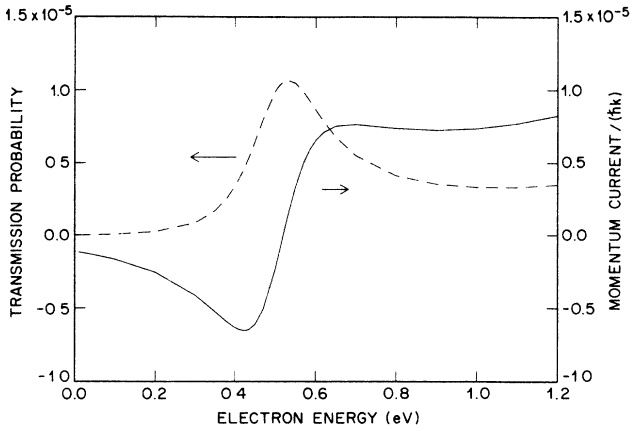

FIG. 6. The transmission probability and the momentum current as a function of electron energy for the barrier of Fig. 5. Note the differing response of the transmission probability (tunneling current) and the momentum current as the electron energy is varied through the atomic resonance. See the text for the parameters characterizing the tunneling barrier.

and

$$M_{22}=-\frac{T_{12}}{T_{11}}. \tag{7.18}$$

Once a_2 and e_1 have been obtained in terms of a_1 and e_2, all the other amplitudes can be obtained using the transfer matrices. By evaluating the expectation value of $\mathbf{J}_p(x)$ at $x=l_2-\epsilon$, one can obtain the momentum current transferred by an electron of energy E as it tunnels to the side of the barrier containing the atom.

Figure 6 shows the mean momentum current and the mean tunneling current as a function of energy E for a monoenergetic beam of electrons that propagate toward the barrier from side 1. Here the parameters $V_a=0$ eV, $V_b=4$ eV, $V_c=-2.1$ eV, $V_d=4$ eV, $V_e=0$ eV, $l_2-l_1=8$ Å, $l_3-l_2=2$ Å, and $l_4-l_3=1.2$ Å were chosen. The tunneling current goes through a maximum when the electron energy matches an energy eigenstate of the atom. The mean momentum transferred is negative for electron energies below the atomic resonance energy and goes through zero at the atomic resonance energy. The momentum transferred approximates the derivative of the tunneling current near resonance. One sees that information independent of that contained in the tunneling current can be obtained from momentum-transfer measurements. A tunneling probe engineered to measure momentum transfer would allow one to look at the exchange or covalent-bonding forces and thus would allow one to look at the chemical properties of a surface.

VIII. CONCLUSIONS

We have shown how to calculate the momentum transfer resulting from electrons tunneling across a vacuum gap. Although the analysis was carried out in one dimension for particles satisfying the free-electron dispersion relation, the techniques should be generalizable to more realistic three-dimensional models. We have shown

that a position-momentum uncertainty product equal to $\hbar/2$ can, in principle, be achieved. This suggests that appropriately engineered tunneling probes can serve as position transducers performing close to the limit imposed by quantum mechanics. If, as Bocko *et al.*[1] have suggested, a tunneling probe can be made sensitive enough to detect momentum transfer, then such an instrument can be used to measure covalent-bonding forces between the electrodes and thus obtain information about the chemical properties of the surface. It should also be noted that if one tunnels into a sufficiently loosely coupled object, such as an organic molecule on a substrate, the momentum noise can induce significant fluctuations in the molecule. For instance, a molecule with a mass of 10^3 amu will have position fluctuations which are comparable to the 0.01-Å position sensitivity of current microscopes.

[1]M. F. Bocko, K. A. Stephenson, and R. H. Koch, Phys. Rev. Lett. **61**, 726 (1988).
[2]G. Binning, H. Rohrer, Ch. Gerber, and E. Weibel, Phys. Rev. Lett. **49**, 57 (1982).
[3]G. Binning, C. F. Quate, and Ch. Gerber, Phys. Rev. Lett. **56**, 930 (1986).
[4]M. Niksch and G. Binning, J. Vac. Sci. Technol. A **6**, 470 (1988).
[5]S. L. Tang, J. Bokor, and R. H. Storz, Appl. Phys. Lett. **52**, 188 (1988).
[6]J. Mamin, E. Ganz, D. W. Abraham, R. E. Thomson, and J. Clark, Phys. Rev. B **34**, 9015 (1986).
[7]N. D. Lang, Phys. Rev. B **34**, 5947 (1986).
[8]G. Doyen, D. Drakova, E. Kopatzki, and R. J. Behm, J. Vac. Sci. Technol. A **6**, 327 (1988).
[9]C. Noguera, J. Microsc. **152**, 3 (1988).
[10]J. Tersoff and D. R. Hamann, Phys. Rev. B **31**, 805 (1985).
[11]J. Bardeen, Phys. Rev. Lett. **6**, 57 (1961).